Instantaneous Scale of Fluctuation Using Kalman-TFD and Applications in Machine Tool Monitoring

P.G. Madhavan[1]

Predictech
3347 Landings Drive
Ann Arbor, MI 48103-2771
email: pgmadhav@eecs.umich.edu

ABSTRACT

A new theory of random fields based on the concept of local averaging was developed in the 80's where the second-order properties of the random fields are characterized by the variance function. Certain asymptotic properties of the variance function lead to the definition of a scalar called the "scale of fluctuation", which has many interesting properties. A non-parametric method of estimating instantaneous scale of fluctuation is developed using the time-varying model-based time-frequency distribution. A wide range of random processes can be modeled by appropriate state-space models with white process noise. For properly defined state transition matrices and observation vectors, the states estimated using Kalman filtering or smoothing algorithms provide the estimated time-frequency distribution (Kalman-TFD). Using Kalman-TFD, the instantaneous scale of fluctuation is estimated. Performance of this estimator is compared to other instantaneous and block methods using the coefficient of variation of the estimators. The Kalman-TFD-based scale of fluctuation estimator has a coefficient of variation of 6% where as other methods yield coefficients of variation greater than 35%. The instantaneous scale of fluctuation quantifies the temporal variability of the underlying system and possible resultant limit-cycle oscillations. Tests with real vibration data from machine tools before and during chatter show that the estimated instantaneous scale of fluctuation may permit on-line prediction of chatter development many hundreds of milliseconds in advance. To explain the behavior of the estimated instantaneous scale of fluctuation during pre-chatter period, detailed simulations were undertaken which revealed that the random process during pre-chatter condition goes through an increase in "degrees-of-freedom" or its unit standard deviation contour volume.

Keywords: random field theory, scale of fluctuation, time frequency distribution, Kalman filtering, machine tool monitoring, chatter phenomenon.

---

[1]Currently at Biocontrol Technology, Inc., Indiana, PA.

SPIE Vol. 3162 • 0277-786X/97/$10.00

1. INTRODUCTION

Vanmarcke [10] introduced a comprehensive theory of random fields which extends very elegantly to multi-dimensional cases. His "random field theory of local averages" captures the effect that local averaging has on a homogeneous random field. The quantification of the effects of local averaging leads to a function which characterizes the second-order properties of the random field called the "variance function". A scalar called the "scale of fluctuation" derived from the variance function has many nice interpretations, some historic and some new. The scale of fluctuation can be considered to be similar to other scalars derived from multidimensional probability density functions such as correlation or Shannon entropy. The information that the scale of fluctuation provides is different from other familiar scalars such as correlation or entropy; in the case of a time series, the scale of fluctuation is a measure of the "time scale" of a random process over which the correlation structure of that random process is characterized [9, 10].

In this paper, it is shown that in the case of Gaussian random process, an invariance property of the scale of fluctuation captures the "volume" characterizing the joint probability density function which may have significant practical applications. A simulated data example is discussed later to develop the ideas behind the invariance property. An important notion of *time-varying* scale of fluctuation is introduced and a new estimation method using Kalman filtering is developed. Performance of this estimator is compared to spectrogram as well as block methods such as those based on AR modeling and periodogram. Analysis of simulated machine-tool vibration data provide the rationale for the use of time-varying scale of fluctuation for the prediction of machine-tool chatter. The paper concludes with preliminary results from the practical application of time-varying scale of fluctuation for the prediction of machine-tool chatter.

2. THEORY OVERVIEW

Consider a zero-mean, stationary, real random process, X(t) with a variance of σ^2 and the following definitions of its second-order properties.

1) Correlation Function:

$$B(\tau) = E[X(t)X(t+\tau)]$$

2) Normalized Correlation Function:

$$\rho(\tau) = \frac{B(\tau)}{\sigma^2}$$

3) Spectral Density Function (s.d.f.):

$$S(\omega) = \frac{1}{2\pi}\int_{-\infty}^{\infty} B(\tau)e^{-j\omega\tau}d\tau$$

4) One-sided s.d.f.:

$$G(\omega) = 2S(\omega)\ ; \qquad \omega \geq 0$$

5) Normalized s.d.f (unit area):

$$g(\omega) = \frac{1}{\sigma^2}G(\omega)$$

The concept of variance function is developed by considering the following moving average process, $X_T(t)$.

$$X_T(t) = \frac{1}{T}\int_{t-\frac{T}{2}}^{t+\frac{T}{2}} X(u)\,du$$

For larger averaging window, T, the variance, σ_T^2, of the corresponding moving average process will be smaller than σ^2. The variance function is defined as follows.

$\gamma(T) = \sigma_T^2 / \sigma^2$

Vanmarcke showed that as T increases, $\gamma(T)$, has a characteristic shape and that the limiting value of $T\gamma(T)$ is very meaningful. In fact, the limit is called the "scale of fluctuation, θ" and the limit exists [10] if the slope of the normalized spectral density function at $\omega=0$ is zero.

$$\theta = \lim_{T\to\infty} T\gamma(T) = \int_{-\infty}^{\infty} \rho(\tau)\,d\tau = \pi g(0) \qquad (1)$$

From equation (1), θ is the "area" under the normalized correlation function or proportional to the zero-frequency ordinate of the normalized spectral density function. Many interpretations for θ exist and are variously known as "characteristic length", "correlation length" or "duration of persistence of trends". For a real-valued, discrete-time autoregressive random process, X(n), of order P, using results developed by Vanmarcke [10], the scale of fluctuation, θ_x, can be obtained as follows.

$$\theta_x = \theta_w \frac{\sigma_w^2}{\sigma_x^2} |H(0)|^2 = \frac{|H(0)|^2}{\sigma_x^2} \quad where\ |H(0)|^2 = \left[\frac{1}{1+\sum_{i=1}^{P} a_i}\right]^2 \qquad (2)$$

Here, $H(\omega)$ is the transfer function of the linear-time invariant system relating white noise process to the AR(P) process, θ_w is the scale of fluctuation of the white noise process ($\theta_w = 1$), σ_w^2 is the variance of the white noise process ($\sigma_w^2 = 1$), σ_x^2 is the variance of the AR(P) process and $\{a_i\}$, i=1 to P are the AR coefficients.

To develop a better understanding of θ, consider two discrete-time AR(2) processes with model equations as follows - (1)$AR_1(2)$: $x_1(n) = 1.8x_1(n-1) - 0.82\,x_1(n-2) + w_1(n)$ and (2) $AR_2(2)$: $x_2(n) = 0.6x_2(n-1) - 0.2\,x_2(n-2) + w_2(n)$. Typical 100-point data sequences are shown in figure 1. Using equation (2), the scale of fluctuation can be calculated knowing that [4],

$$\sigma_x^2 = \frac{1+a_2}{1-a_2}\,\frac{1}{(1+a_2)^2 - a_1^2} \qquad (3)$$

where a_1, a_2 are the AR coefficients {-1.8, 0.82} and {-0.6, 0.2}. For $AR_1(2)$, $\theta_1 = 17.9$ and for $AR_2(2)$, $\theta_2 = 2$. The interpretations of θ as "correlation length" or "duration of persistence of trends" are clear by considering the plots in figure 1. From the plotted data, the $AR_1(2)$ process can be seen to be narrow-band with a correlation function that will presist for a long time ($\theta_1 = 17.9$) whereas the $AR_2(2)$ process has a correlation function that dies out rapidly ($\theta_2 = 2$).

3. INVARIANCE PROPERTY

For a real-valued AR(2) process, consider the expression for θ. If the pole positions corresponding to real coefficient $\{a_1, a_2\}$ are $(x \pm jy)$, the expression for θ can be written as follows.

$$\theta = \frac{(1-x^2-y^2)[(1+x^2+y^2)^2-4x^2]}{(1+x^2+y^2)[(1-2x+x^2+y^2)^2]} \qquad (4)$$

The "θ = 1" constant-θ contour is plotted in figure 2(a). It shows the plot in the first quadrant of the z-plane with a semi-cirle for comparison. By setting θ = 1 in equation (4), we obtain the quartic equation, $(x^2 + y^2)^2 + x^2 + y^2 - 2x = 0$, shown in figure 2(a). For comparison, the circle shown in figure 2(a) has the quadratic equation, $(x - ½)^2 + y^2 = (½)^2$. If we consider the θ = 1 contour approximately circular, in figure 2(b), we can see that constant-θ contours for θ >1 are approximate circles of smaller diameter and with centers along the real axis closer to the unit circle. Any pole pairs that lie on the same constant-θ contour will have different $\{a_1, a_2\}$ coefficients but the same θ. For example, consider the two AR(2) processes marked on the θ=3 contour in figure 2 (only the pole in the first quadrant is marked). The first process, $AR_A(2)$, has poles at (0.9 ± j0.26) and the second process, $AR_B(2)$, has poles at (0.35 ± j0.17). The corresponding AR coefficients are {-1.8, 0.8776} and {-0.7, 0.154} respectively. Typical 100-point data sequences are shown in figure 3. As is clear, $AR_A(2)$ and $AR_B(2)$ are very different processes with different correlation functions (or spectral densities), yet the same θ. The significance of this *invariance property* will become clearer when we consider its practical application in the case of machine-tool chatter signal analysis and realted simulation studies.

At this time, it not clear what invariant *physical property* of the random process is being captured by the scale of fluctuation. However, it is interesting to consider further the linear time invariant system in the modeling of AR processes. In this simple, second order linear system case, we can compare the constant-θ contour to other traditional contours such as constant-ξ (damping ratio) and constant-ω_n (natural frequency) contours [3]. The constant-ξ contours are logarithmic spirals and the constant-ω_n contours are at right angles to the logarithmic spirals, both distinctly different from the constant-θ contour. Our conjecture is that all Gaussian random processes that lie on the constant-θ contour have similar unit-standard deviation contour volume. This possibilty will be explored further for the case of simulated machine-tool chatter signal analysis.

4. TIME-VARYING "θ" OF DISCRETE-TIME SIGNALS

By extending equation (1) using the time-varying normalized spectral density function, g(ω,t), a time-varying θ can be defined as being proportional to the zero-frequency ordinate of the normalized time-varying spectral density function, i.e., θ(t) = π g(0,t).

In recent years, significant advances have occured in the field time-varying spectra or "time-frequency distributions" [1]. The time-frequency distributions (TFDs) allows one to estimate the power spectral density as it varies over time, primarily for deterministic signals. These concepts have been extended to random signals by the development of time-varying model based TFD or "TVM-TFD" [6].

Consider a general state space model of a time-varying stochastic discrete-time signal, y(n), as given below.

$$\underline{X}(n+1) = \underline{A}_n \underline{X}(n) + \underline{w}(n); \quad \underline{X}(n) = [X_1(n) \; . \; . \; X_k(n) \; . \; . \; X_M(n)]^T \qquad (5a)$$

$$y(n) = \underline{\Phi}_n^T \underline{X}(n) + e(n); \quad \underline{\Phi}_n = \frac{1}{M}\left[1 \; . \; . \; e^{j\frac{2\pi}{M}nk} \; . \; . \; e^{j\frac{2\pi}{M}n(M-1)}\right]^T \qquad (5b)$$

For arbitrary choice of the matrix, $\underline{A}_n$, and the vector, $\underline{\Phi}_n$, equations (5a), (5b) is sometimes referred to as a time-variable parameter (TVP) model of a stochastic time series [11]. In the noise-free observation case, y(n) can be written as follows.

$$y(n) = \underline{\phi}_n^T \underline{X}(n) = \frac{1}{M}\sum_{k=0}^{M-1} e^{j\frac{2\pi}{M}nk} X_k(n) \qquad (6)$$

Equation (6) can be seen to be the Goertzel algorithm [8] where $X_k(M)$ is the k^{th} coefficient of the M-point DFT of the finite-duration sequence $\{y(n), 0 \le n \le (M-1)\}$ and $\underline{X}(n)$ is the vector, elements of which are the M-point DFT coefficients, $X_k(M)$, k=1 to M. To define a time-varying spectrum based on $\underline{X}(n)$, we proceed as follows.

In equation (5), assume that e(n) and $\underline{w}(n)$ are zero-mean Gaussian white noise sequences such that $E[e(k)\,\underline{w}(l)] = \underline{0}$ for all k and l and the initial "state" $\underline{X}(0)$ is independent of e(k) and $\underline{w}(l)$. In the case where N samples of y(n) are available, $\underline{X}(n)$ can be estimated by Kalman filtering algorithm [5, 11]. Specifically, given a noisy observation, y(n), the Kalman filter computes estimates $\underline{X}(n)$ of the DFT coefficients at time n. The variations of the DFT coefficients over time can be used to estimate the time-frequency distribution [1]. We define the time-varying model based time-frequency distribution (TVM-TFD) as

$$S(k,n) = |X_k(n)|^2 \quad for\ n,k = 1,2,...N \qquad (7)$$

The TVM-TFD, S(k,n), estimates the power spectral density at discrete frequency, k and discrete time, n. Based on the TVM-TFD, we define an estimate of the time-varying scale of fluctuation, T(n), as follows.

$$T(n) = \frac{S(0,n)}{r(0,n)} \qquad (8)$$

Here, r(m,n) is the instantaneous autocorrelation sequence and r(0,n) is the instantaneous mean-squared value of the discrete-time random process, y(n). Note that the normalizing factor, π, does not appear in equation (8) because of the definition of time-varying spectral density in equation (7).

5. PERFORMANCE COMPARISON OF ESTIMATORS

The performace of Kalman-TFD-based estimator of the scale of fluctuation as given in equation (8) is compared to a spectrogram-based estimator (spectrogram replaces S(0,n) in equation 8) in figure 4. The T(n) was estimated over ten 100-point segments and the average for each segment in shown in figure 4. As a performance index, the coefficient of variation (standard deviation ÷ mean) was calculated for the spectrogram-based and Kalman-TFD-based estimates. The coefficient of variations of 83.6% and 6.0% respectively were obtained which shows the significant superiority of of the Kalman-TFD-based estimator. Additional comparisons were made to "block" methods where θ was repeatedly estimated over 100-point segments using the AR-model based method (given by equation 2) and periodograms. Vanmarcke [10] has also provided a theoretical estimate of the coefficient of variation of the sample autocorrelation function-based estimate which can be used as the basis for all comparisons. The results are tabulated in Table 1. The superiority of the Kalman-TFD-based estimator of θ is clearly evident.

Table 1. Comparison of Scale of Fluctuation Estimators

Estimator Type		Coefficient of Variation
Instantaneous	Kalman-TFD	6%
	Spectrogram	84%
Block	AR Model-based	80%
	Periodogram	35%
Theoretical	Sample Correlation Function	115%

6. TIME-VARYING "θ" - SIMULATION STUDIES

The properties of the estimate of the time-varying scale of fluctuation, T(n), will closely resemble the properties of the TVM-TFD [6]. The use of Kalman filtering for TVM-TFD assures optimality of estimates in the mean-square sense which translates into good noise performance. The good localization and cross-term properties of the TVM-TFD results in S(0,n) being a good time-varying estimate of the zero-frequency ordinate of the time-varying spectral density function. In this section, we demonstrate some of these properties through simulation studies. The simulation data are chosen with the additional aim of providing a basis for the explanation of real data tests to be undertaken in Section 7.

The pole positions of the three AR(2) processes are shown in figure 5. The processes are (1) AR_1, with poles at $(0.6 \pm j0.095)$ and corresponding AR coefficients {-1.2, 0.369}, (2) AR_2, with poles at $(0.6 \pm j0.46)$ and corresponding AR coefficients {-1.2, 0.5716} and (3) AR_3, with poles at $(0.95 \pm j0.14)$ and corresponding AR coefficients {-1.9, 0.9221}. The θ of the three processes are calculated by equation(2) and marked on the constant-θ contours in figure 5. The θ for AR_1, θ_1 and AR_3, θ_3 are equal ($\theta_1 = \theta_3 = 7$) whereas for AR_2, $\theta_2 = 2$. The figures 6 (a), (b) and (c) show a realization of 1000 points each of the three time series as well as plots of the estimates of the time-varying scale of fluctuation, T(n), for each time series. By visual inspection of the time series plots, it can be seen that the time-domain (amplitudes) and frequency-domain (broad-band nature) features of AR_1 and AR_2 are very similar and AR_3 is most dissimilar whereas T(n) of AR_1 and AR_3 are similar (estimate close to the theoretical value of 7) and AR_2 is most dissimilar (estimate close to the theoretical value of 2). It can be observed that T(n) "tracks" the theoretical θ value for the three processes quite closely. The mean values of T(n) (shown by dotted horizontal line) in figures (a), (b) and (c) are 7.2, 2.2 and 6.6, showing good agreement with the theoretical θ values.

Comparing figure 6 (a) and (c), it is striking to note that whereas their θ values are equal (= 7), the appearence of the time series is quite different. The AR_3 series is over 5 times in amplitude compared to AR_1. The AR_3 series is also quite band-limited compared to the broad-band nature of AR_1 . Note that these features are entirely consistent with the pole positions shown in figure 5 for these two processes. Conversely, from figure 6 (a) and (b), it is striking to note that whereas their θ values are different (7 and 2, respectively), the appearence of the time series is quite similar. This leads to the conclusion that θ captures some property of the random process different from its first or second order statistical properties. In other words, even though the definition of θ is based on the autocorrelation or spectral density function, θ may capture one (or some small set of) specific feature of the joint probability density function. The intuition related to the real-data application to be discussed in Section 7 leads to the possibility that the specific feature that θ captures may be related to the volume of the unit standard deviation contour of the joint probability density function. We explore this possibilty as follows.

Consider an n-dimensional random vector, y, representing a Gaussian discrete-time random process. The joint probability density function of y is given by the following equation.

$$f(y) = \frac{1}{2\pi |C|^{\frac{1}{2}}} \exp\left[-\frac{1}{2} (y-\mu)^T C^{-1} (y-\mu) \right] \qquad (9)$$

Here, μ is the mean vector and C is the autocovariance matrix. For the zero-mean case, the unit standard deviation (u.s.d.) contour is given by the equation, $y^T C^{-1} y = 1$ [see 2, for example]. In the 2-dimensional case, the equation is that of an ellipse with the semi major and minor axes equal to the square roots of the eigenvalues of C, the autocovariance matrix [2]. The volume, V, of the unit standard deviation contour (a hyper-ellipse) is given by the following equation where λ_n is an eigenvalue of C and there are K significant eigenvalues.

$$V \propto \prod_{n=1}^{K} \lambda_n^{1/2} = D \qquad (10)$$

In our simulation studies, the u.s.d. contour volumes were estimated for the three random processes from each of their (100x100) averaged, normalized autocovariance matrices. In figure 7, the largest 50 eigenvalues in descending order are plotted for AR_1, AR_2 and AR_3. It can be seen that the number of significant eigenvalues are different for each process. The selection of the number of significant eigenvalues is generally problematic. To aid in the selection process, we proceeded as follows. For AR_1 and AR_3 in figure 7 (a) and (c), we calculated the "change of slope" of the ordered eigenvalues to aid in the detection of the "knee" in the eigenvalue profiles. The largest index for which the change of slope was greater that one was judged to be the location of the knee, provided that the magnitude of the eigenvalue at the knee was significantly less (50% or less) than the first eigenvalue. The number of significant eigenvalues (index number, K) was chosen as one index number less than the knee location. Such a procedure yielded values of 7 and 6 for AR_1 and AR_3. For AR_2 in figure 7 (b), a "knee" is not detectable based on the above criterion; K was chosen as 25 at which a sudden change of the magnitude of the eigenvalue can be detected. The u.s.d. contour volume of each joint probability density function is calculated using equation (10) where n is replaced by K for that random process.

Table 2- Comparison of Unit Standard Deviation Contour Volume

AR Process	θ	K	D
AR_1	7	7	0.64×10^3
AR_2	2	25	0.65×10^6
AR_3	7	6	2.04×10^3

The comparison in Table 2 shows that AR_1 and AR_3 have similar θ, "degrees of freedom" and volumes whereas AR_2 has a volume 3 orders of magnitude larger. This observation justifies the conjucture that θ may capture a measure related to the volume of the unit standard deviation contour. The fact that small θ implies large volume in which the random process exists suggests an intuitively appealing explanation of the results of the real-data application to be discussed in the next section.

7. AN APPLICATION OF TIME-VARYING "θ": PREDICTION OF MACHINE TOOL CHATTER

Machine tool chatter is a self-excited relative vibration between the work piece and the cutting tool in common machining processes such as turning process on a lathe [7]. The presence and evolution of chatter can be monitored by measuring the vibration signals from the cutting tool using appropriately placed accelerometers. Such a signal is called the "chatter signal". The chatter signal can be analyzed to discern the state of the machining process and this information can be used to predict the possible future development of chatter.

In figure 8, the chatter signal and the corresponding estimates of the time-varying scale of fluctuation, T(n), are shown. In figure 8(a), the condition of the machine is "normal operation". It can be noticed that the time series and T(n) are comparable to AR_1 in the simulation studies in Section 6 (compare figures 8(a) and 6(a)). In figure 8(b), the first 300 milliseconds or so is the "pre-chatter" period and the rest is the "fully-developed chatter" period. The "pre-chatter" period is comparable to figure 6(b) and "fully-developed chatter", to figure 6(c).

The following features are important to note in figures 8(a) and 8(b). The amplitude scales for the chatter signal are different; the amplitude in figure 8(a) during normal operation is of the same order as the amplitude of pre-chatter signal in the interval from 0 to 250 msec in figure 8(b). In figure 8(a), the value of T(n) stays relatively stable around 7. In figure 8(b), when chatter is fully developed after 450 msec, T(n) value is again approximately around 7. Thus T(n) is *relatively insensitive* to operating conditions during normal operation and fully developed chatter. In figure 8(a), the value of T(n) is significantly and consistently below 5 during pre-chatter condition. It can be concluded that the value of T(n) staying below 5 is a predictor of chatter that develops fully after approximately 400 msec.

The reduction of the value of T(n) during pre-chatter period as a predictor of future chatter development can be explained in the light of observations made in Section 6. The random process during pre-chatter condition behaves similar to AR_2 in Section 6, which as shown in Table 2, goes through an increase in "degrees-of-freedom"

and its u.s.d. contour volume. This expansion of the machine system's *phase-space* makes it vulnerable to getting trapped in certain fundamental modes of the system which will result in energy build up in a narrow frequency range and resultant nonlinear limit cycle type of oscillations characteristic of chatter.

8. CONCLUSIONS

The invariance property of scale of fluctuation, θ, for certain class of random processes was introduced. For second-order auto-regressive random processes, it was shown that constant-θ contours are approximately circles with centers on the non-negative real axis with radius less than or equal to half. It should be noted that the invariance property of θ discussed in this article is distinct from a quantity Vanmarcke has defined as "invariant-θ" of a random process which is the product of the variance and the θ of the random process [10]. It can also be seen that in the second order system case, the contours of constant "invariant-θ" is quite different from the approximately circular constant θ contours discussed in this article.

A Kalman filter based non-parametric method of estimating time-varying θ was developed using the time-varying model-based time-frequency distribution. Simulated data showed that θ captures a very important invariant property related to the unit-standard deviation contour volume of the joint probability density function of the Gaussian random process. Tests with real vibration data from machine tools before and during chatter show that estimated θ may permit on-line prediction of chatter development many hundreds of milliseconds in advance.

ACKNOWLEDGEMENTS

The author would like to thank Professor E. Vanmarcke of Princeton University for reviewing a preprint of this article. The author is very grateful to Dr. P. Chalmer of the National Center for Manufacturing Sciences for discussions on many specific issues in this paper. Appreciation for providing some real machine tool data is expressed to Professor J. Ni of the University of Michigan, Ann Arbor.

REFERENCES

[1] Cohen, L., *Time Frequency Analysis*, Prentice-Hall, New Jersey, 1995.
[2] Duda R.O. and Hart, P.E., *Pattern Classification and Scene Analysis*, John Wiley, NY, 1973.
[3] Franklin, G.F. and Powell, J.D., *Digital Control of Dynamic Systems*, Addison-Wesley, MA,1981.
[4] Haykin, S., *Adaptive Filter Theory*, 3rd edition, Prentice-Hall, New Jersey, 1996.
[5] Kalman, R.E., "A New Approach to Linear Filtering and Prediction Problems", *ASME Trans., J. Basic Eng.*, vol. 83-D, pp 95-108, 1960.
[6] Madhavan, P.G. and Williams, W.J., "*Kalman Filtering and Time-Frequency Distribution of Random Signals*", Proceedings of the Society of Photo-Optical Instrumentation Engineers (SPIE) 1996 Conference, Denver, CO, 1996.
[7] Minis, I.E., Magrab, E.B. and Pandelidis, I.O., "Improved Methods for the Prediction of Chatter in Turning, Part 3: A Generalized Linear Theory", ASME *Journal of Engineering for Industry*, vol. 112, pp 28-35, 1990.
[8] Oppenheim, A.V. and Schafer, R.W., *Discrete-Time Signal Processing*, Prentice Hall, New Jersey, 1989.
[9] Rodriguez-Iturbe, I., "Scale of Fluctuation of Rainfall Models", *Water Resources Research*, vol. 22, pp 15S-37S, 1986.
[10] Vanmarcke, E., *Random Fields: Analysis and Synthesis*, MIT Press, MA, 1988.
[11] Young, P., "Time Variable and State Dependent Modelling of Non-Stationary and Nonlinear Time Series", in *Developments in Time Series Analysis*, Subba Rao, T. (ed), Chapman & Hall, London, 1993.

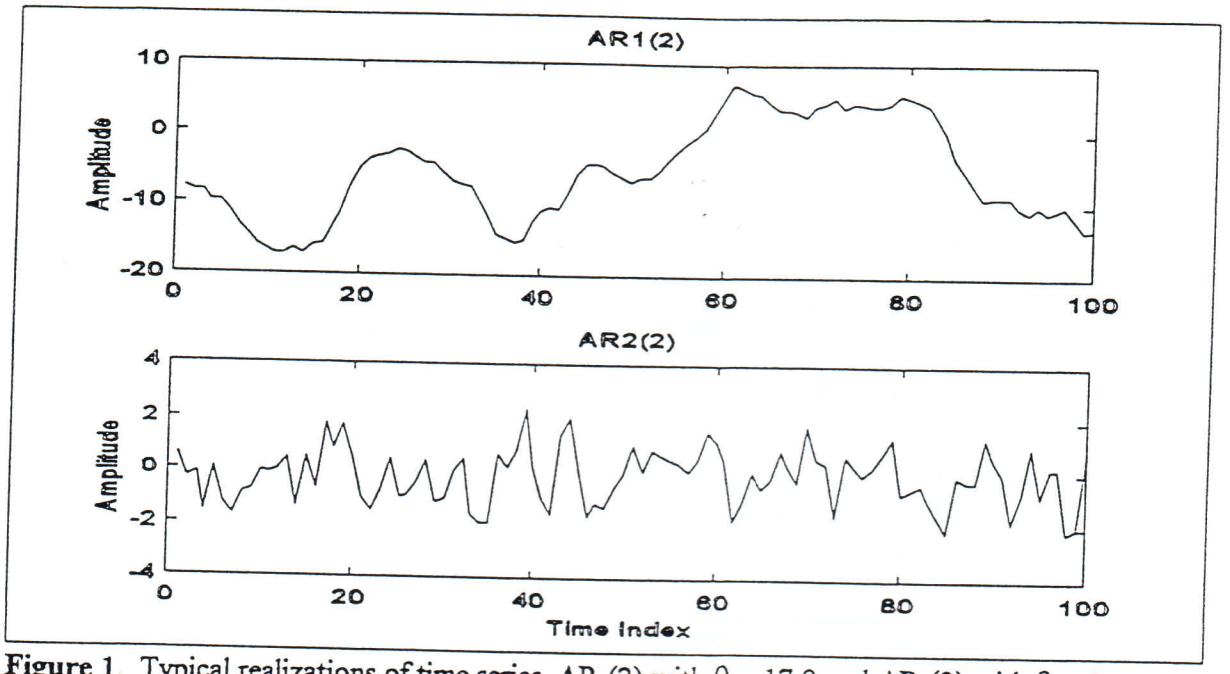

Figure 1. Typical realizations of time series, $AR_1(2)$ with $\theta = 17.9$ and $AR_2(2)$ with $\theta = 2$.

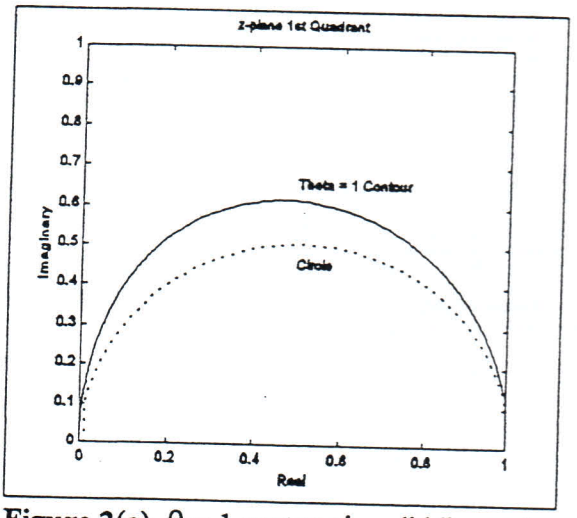

Figure 2(a). $\theta = 1$ contour in solid line and circle, $x^2 + y^2 = x$ in dotted line.

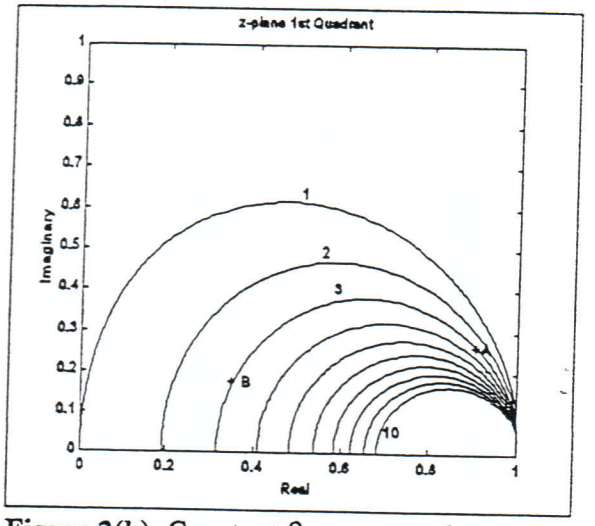

Figure 2(b). Constant θ contours; the two AR(2) random processes, A and B, are marked on the $\theta = 3$ contour.

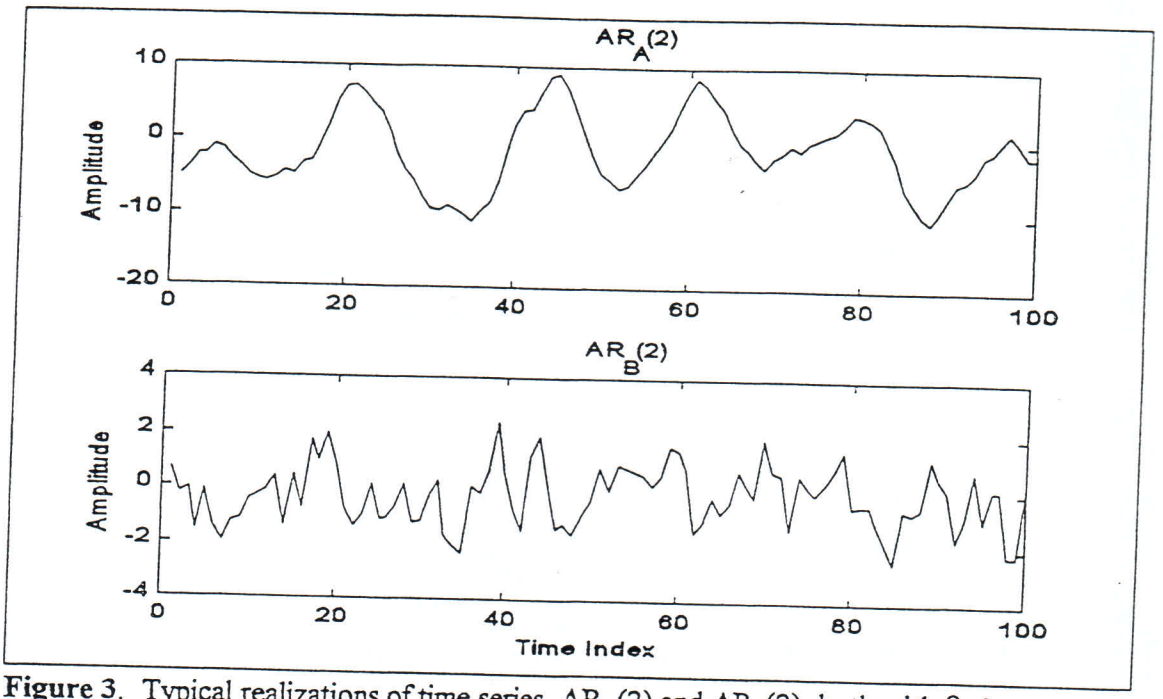

Figure 3. Typical realizations of time series, $AR_A(2)$ and $AR_B(2)$, both with θ=3.

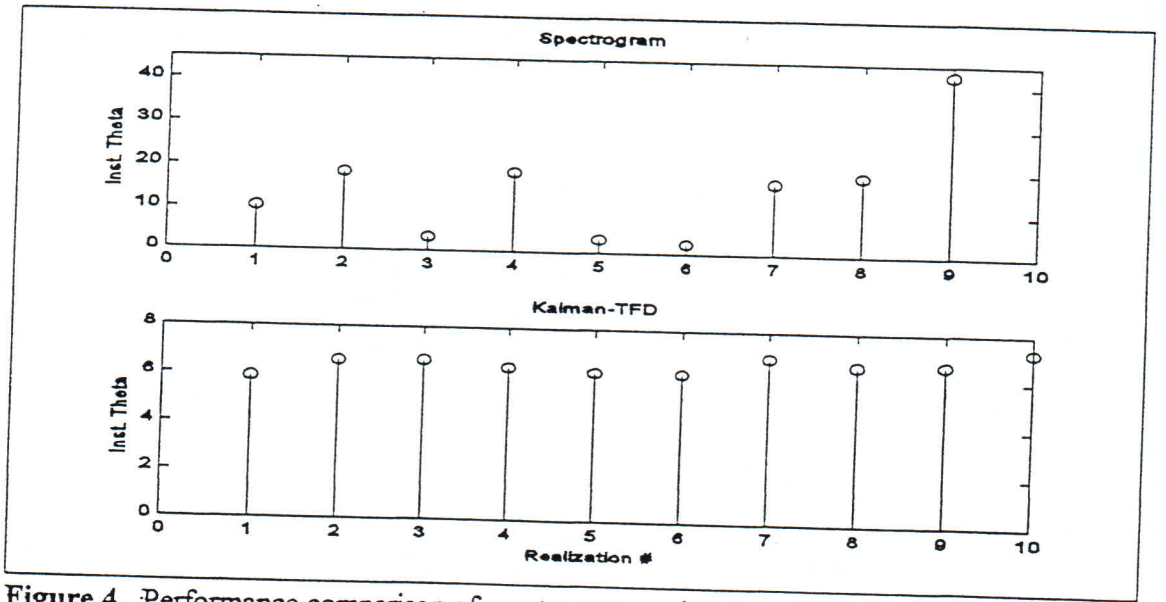

Figure 4. Performance comparison of spectrogram and Kalman-TFD-based estimators of instantaneous scale of fluctuation. Spectrogram: coefficient of variation = 83.6%. Kalman-TFD: coefficient of variation = 6.0%.

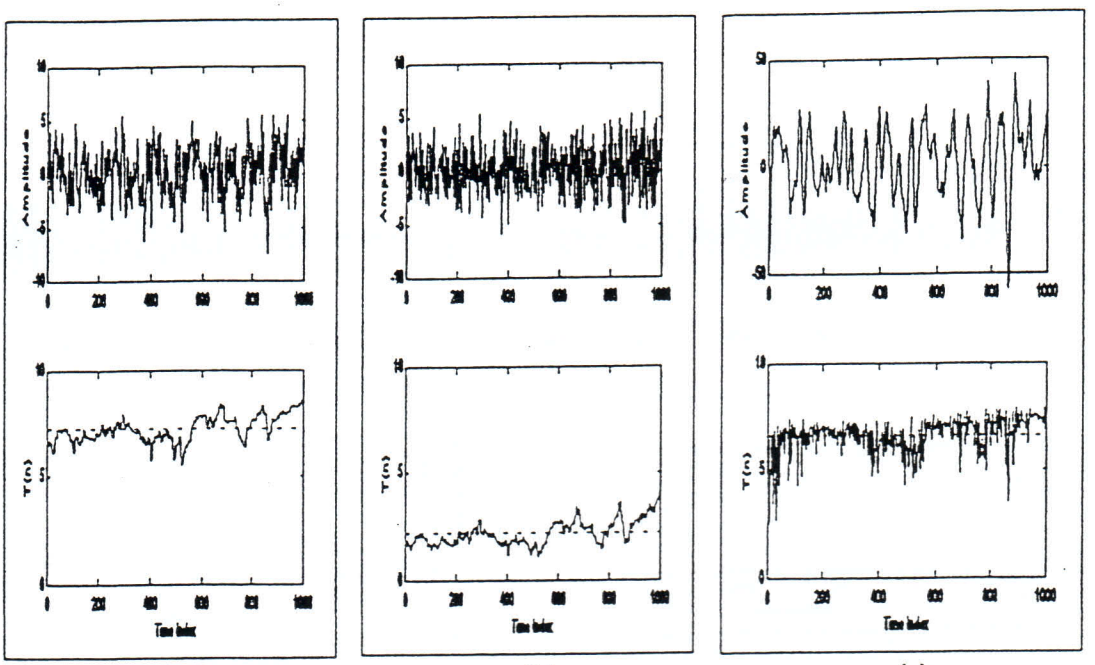

Figure 6. Results of simulation studies involving 3 AR(2) processes; AR_1 with $\theta_1 = 7$, AR_2 with $\theta_2 = 2$ and AR_3 with $\theta_3 = 7$. Typical realizations are shown in the top row and time-varying scale of flcutuation estimates in the bottom row. Mean values of T(n), shown as dotted horizondal lines, are 7.2, 2.2 and 6.6 for AR_1, AR_2 and AR_3 respectively.

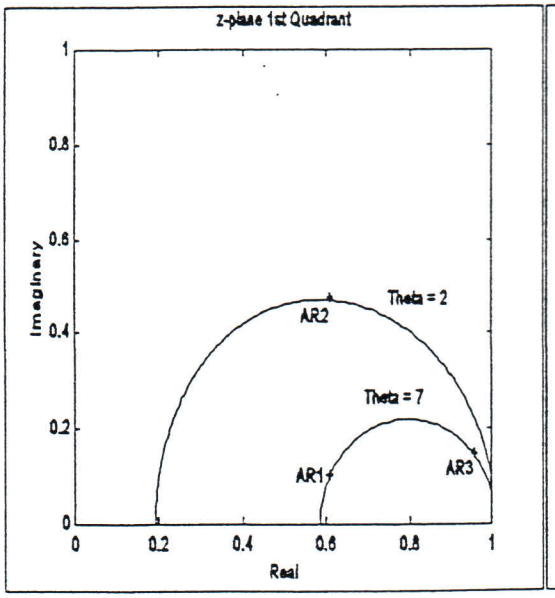

Figure 5. Constant θ contours; AR_1 and AR_3 on θ = 7 contour and AR_2 on θ = 2 contour.

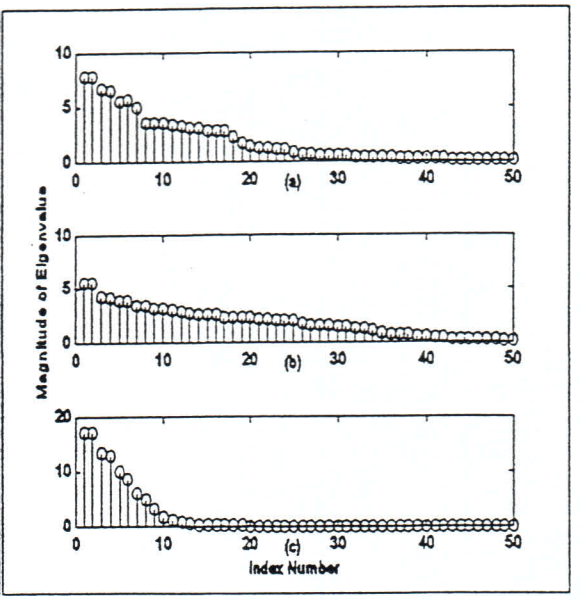

Figure 7. Eigenvalues of the averaged normalized autocovariance matrices of AR_1, AR_2 and AR_3 in (a), (b) and (c), respectively.

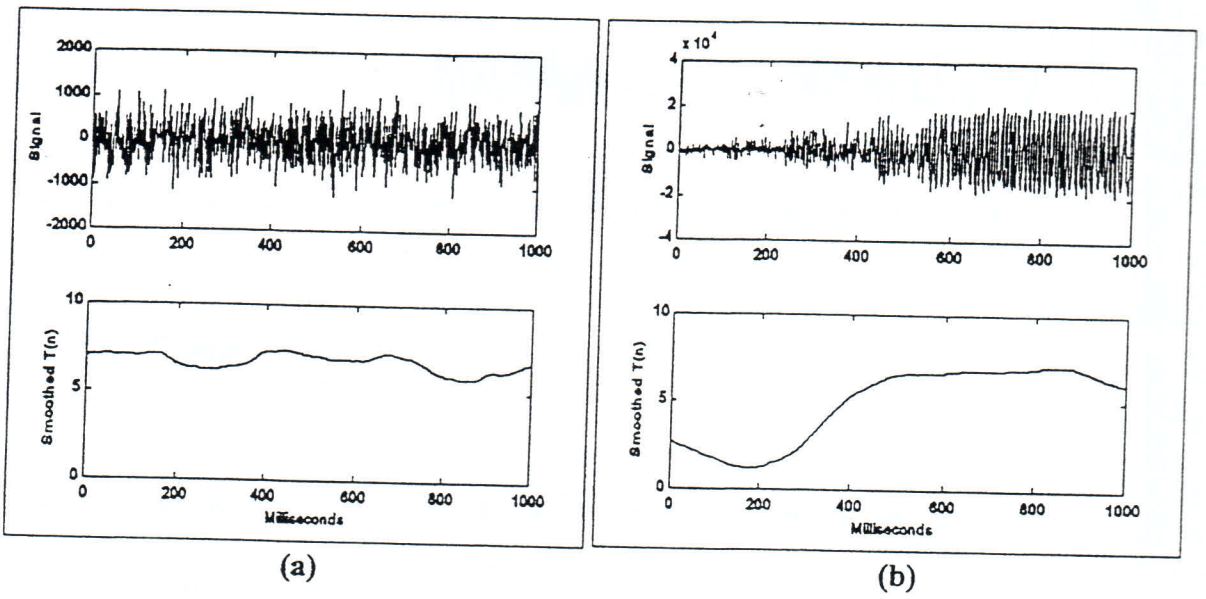

Figure 8. (a) Real data test during normal operation- NO CHATTER condition (note: chatter signal amplitude scale different in (a) and (b)); (b) Real data test during various chatter conditions: (1) pre-chatter from 0 to 250 msec; (2) chatter onset from 250 to 450 msec and (3) fully developed chatter from 450 msec to 1 sec.